Advances in Thermal Processes and Energy Transformation
Volume I, 2018, Bert01, pp. 01-04
ISSN 2585-9102

Ash ring formation in lime rotary kilns

René Berta[1] ● Ladislav Lukáč[2]

[1]Department of Thermal Engineering and Gas industry, Technical university in Košice, Letná 9, 042 00 Košice, Slovakia, rene.berta@tuke.sk
[2]Department of Thermal Engineering and Gas industry, Technical university in Košice, Letná 9, 042 00 Košice, Slovakia, ladislav.lukac@tuke.sk

Category : Original Scientific Paper
Received : 20 February 2018 / Revised: 05 Marec 2018 / Accepted: 17 Marec 2018

Keywords : ash ring, fuel, lime production, rotary kiln,

Abstract : This paper describes in different sections all know factors influencing ash ring formation in lime rotary kilns. Ash ring is mostly influence by fuel and lime properties and its impurities and process conditions. The paper describes different types of ash rings that might formed in rotary kilns. Factors were analyzed from feed batch, fuel to construction parts of rotary kilns. Papers describes all know factors how to prevent ash ring formation and how decrease ash ring formation and its influence on operational conditions of lime rotary kilns.

Citation: Berta, R., Lukáč, L.: Ash ring formation in lime rotary kilns, Advance in Thermal Processes and Energy Transformation Volume I, Nr. I(2018), p. 01-04, ISSN 2585-9102

1 Introduction

Lime production is one of the most important process in industry. Lime has variety of industrial usage in steel production, building, glass, paper industry and for water treatment. Based stone type and fuel availability different types of kilns are used, most common kiln are single haft kilns, parallel flow regenerative kilns and rotary kilns. Rotary kilns are mainly use for lime production in steel industry, where is high lime demand. Rotary kilns for lime production using different fuel types. In Europe most common fuel is coal and natural gas, but more and more frequently alternative fuels are being used. Due to usage of solid fuel with ash content there is specific problem with formation of ash ring, that limits kiln production, operational conditions and kiln availability. [1]

2 Ash ring formation in rotary kilns

Generally, in rotary kiln, firing solid fuels occurs phenomena of ash ring (coating) formation. The ash ring is formed by reaction between impurities coming from feed and ash from fuels in certain range of temperatures. In Figure 1 is example of ash ring formed in lime rotary kiln.

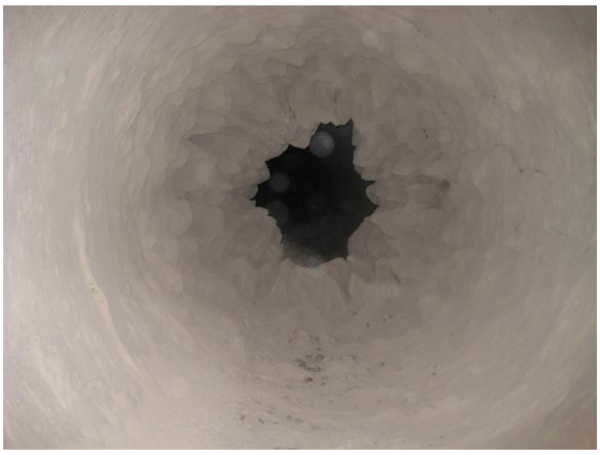

Figure 1 Ash ring in lime rotary kiln

Ash ring formation negatively influences process parameters (kiln pressure loose, kiln load, increase of stone bed depth, etc.) and mechanical load of kiln shell, refractories by weight of ash ring. Due to these phenomena kilns has to be more frequently stopped. In lime rotary kiln ash ring is formed in calcination zone. Figure 2 shows kiln temperature profile, are marked has ash ring formed and that cause lower shell temperature. Decrease of temperature marked by blue arrow show kiln tyres ring.

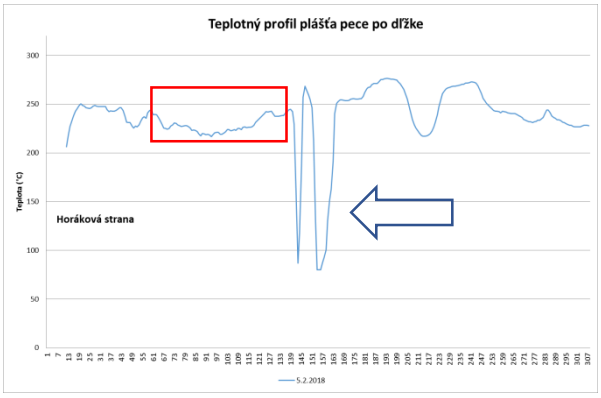

Figure 2 Rotary kiln temperature profile

2.1 *Mechanism of ash ring formation in rotary kilns*

Current research shows that following elements participate on ash ring formation: CaO, SiO_2, Al_2O_3, Fe_2O_3, MgO, SO_3, Cl, K_2O, Na_2O.

In case of lime rotary kilns is ring formed with particles on alumina bases. Ash ring has usually high mechanical strength that is caused by precipitation and sintering of particles forming the ash ring. Liquid phase is partially formed by sintering of alumina and iron phase. Ash ring formation is influenced by composition of alternative fuels, increase amounts of alternative fuels tends to promote ash ring formation in comparison to natural gas and low ash content coal. Alumina phase brought by feed to kiln has critical impact on ash ring formation. Figure 3 show phase diagram of mixture CaO-Al_2O_3-Fe_2O_3-SiO_2 with impurities of MgO. Eutectic point indicates starting temperature when preliminary melt is formed with mentioned chemical composition and creates melted mixture. This melt starts to form at 1300°C and 14% vol. Fe_2O_3 in preliminary liquid phase. With decreased Fe_2O_3 content melting temperature of melt is increased.

Ash composition coming from fuel contents high ratio of iron/alumina components, with increased ratio of ash formed from alumina components, decreased melting temperature, that cause at the same temperature higher ash ring formation which in solid phase is cumulated on refractory. This effect could increase with deposit of unburned coarser fuel and local higher temperature with burning of this fuel. With growing ash ring, growth is getting faster due to shorter distance between ash ring and flame and it is closer to hotter flame part.

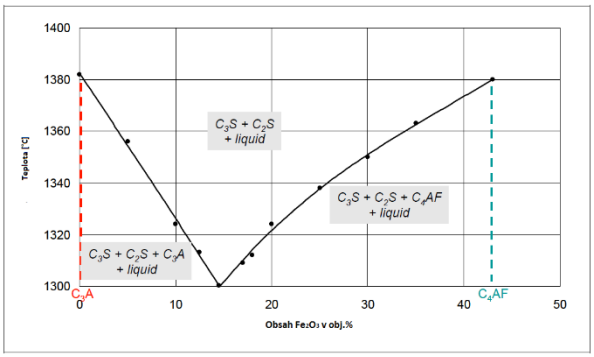

Figure 3 Phase diagrm of CaO-Al2O3-Fe2O3-SiO2 with MgO impurities

On figures 4,5,6 below it is visible growth of ash ring (marked with black arrow) during kiln campaign. Kiln was stopped due to ash ring after 25 days. From second half of campaign is visible that ash ring growth is faster.

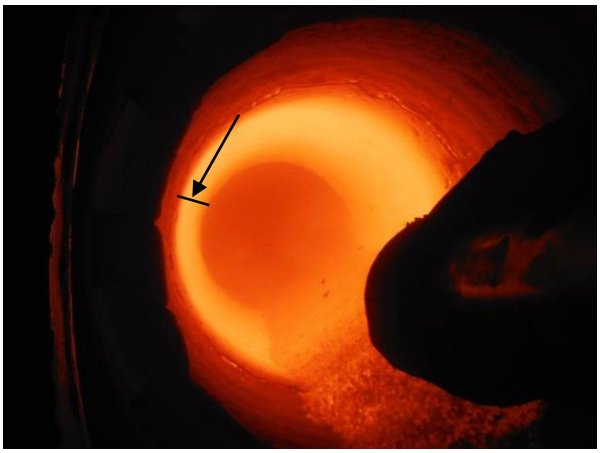

Figure 4 Ash ring size after 11 day of operation

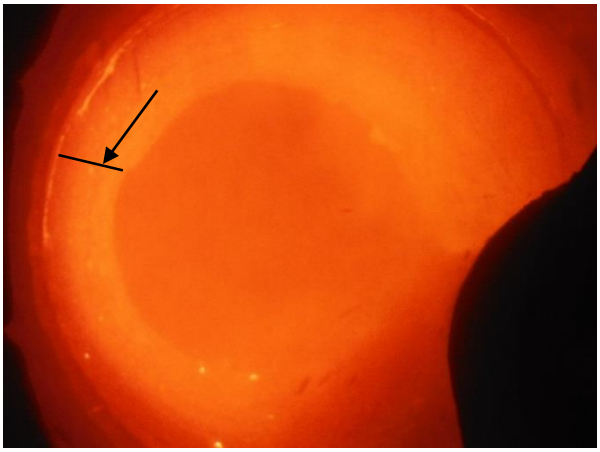

Figure 5 Ash ring size after 19 days of operation

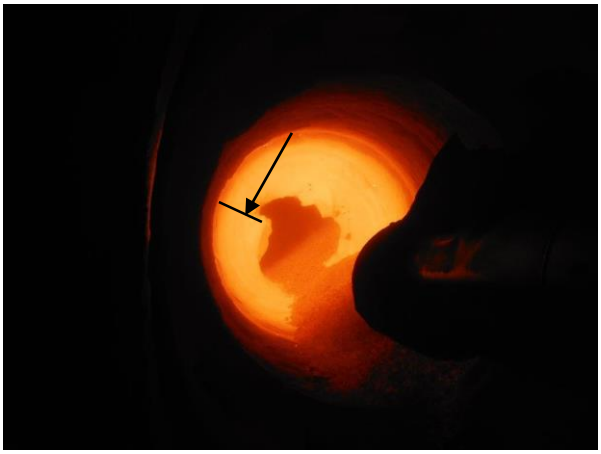

Figure 6 Ash ring size after 23 day of operation

Termovision pictures below show how shell temperature has changed before (Figure 7) and after (Figure 8) ring formation. Big temperature difference demonstrates thickness of ash ring.

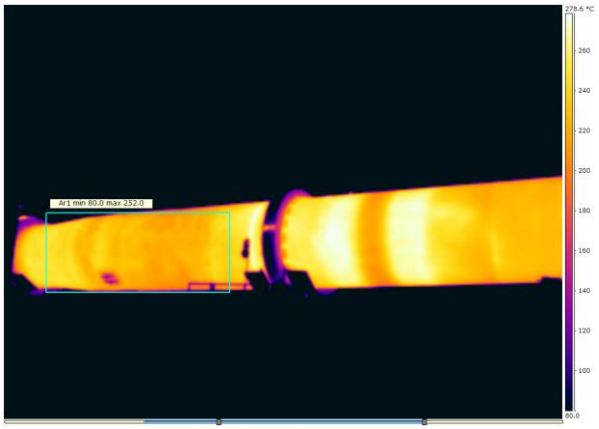

Figure 7 Kiln at begining of campaign without ash ring

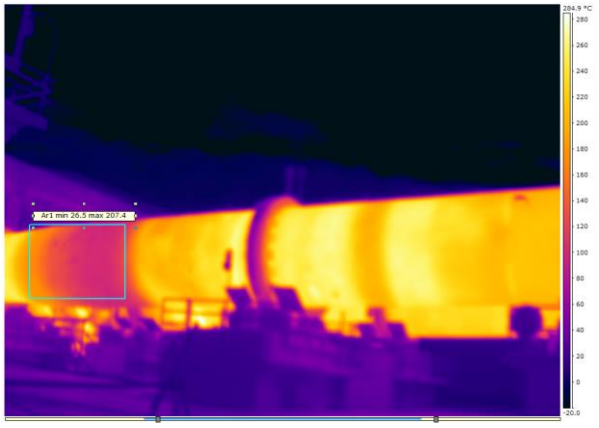

Figure 8 Kiln at end of campaign with ash ring (23 days)

2.2 Location of ash ring in rotary kilns

On pictures below there are marked several locations of ash ring formation in rotary kilns. Location are marked with numbers.

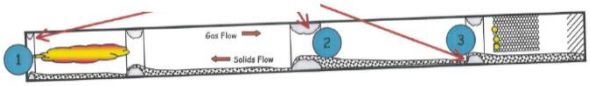

Figure 9 Location of ash ring in rotary kilns 1

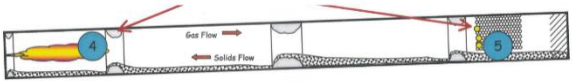

Figure 10 Location of ash ring in rotary kilns 2

1. Dust ash ring – Occasionally forms during kiln start up. Dust is transferred by secondary air from cooler and remains on retention ring. This type of ash ring usually collapse itself during the kiln start-up.
2. Middle- kiln ash ring – Potassium component forms liquid phase in calcination part of kiln. Particles in this section agglomerating together, joints refractory a creates ring. At begging ring is soft and contains $CaCO_3$ and CaO, later when operational condition change, ring is cooled down and CaO reacts with CO_2 and forms $CaCO_3$, this is called re-carbonatation. During this process ring becomes harder and it is not able to fall itself. This is ring is typical for kilns with processing wet calcium mud.
3. Mud rings – Moisture level of mud suppose to be below 5%. In case moisture is above 15% ash ring forms in chain section
4. Ash ring in burning zone- This type of ash ring is in kilns with dry feed and fuels has a lot of ash.
5. Sodium ball – If dust level is above 15% of dry matter entering the kiln, than it is entrained as dust by fumes, then this creates balls on chains.

3 Possibilities of ash ring reduction in rotary kilns

The main driver for ash ring reduction is inputs control. For the lime kiln main feed is limetone with its impurites and different types of solid fuel like a coal,

solid alternative fuels. In this this case to eliminate ash ring formation there are following recommendations:

1. Selection of fuel with proper fuel properties

Based experience there are several parameters influencing the ash ring formation the most. Low fuel fusion temperature is promoting ash ring formation, recommeded softening temperature is 1400°C and fusion temperature more than 2800°C. Maximum avarage ash contend should be below 8,5 % in dry matter. Minimum requirement of ash composition is Fe_2O_3 <8,0 %, Na_2O <1,0 %, K_2O <2,0 %, CaO <2,0 %

2. Stable feed quallity

Cleanest and proper granulometry of the feed is cruicial for decrease of ash ring formation. Lot of impurities like sand, clay, mud brings change of ash and lime kiln dust properties and promotes reaction of lime, that reacts with ash and sinters on the wall of kiln.

3. Process control

The main driver for the process control is to reduce reduction atmosfere in kiln. It is crucial to have good mixing of fuel and air to reduce alternative fuel to fall on bed. This is possible to improve by sufficient swirl effect and burner momentum.

4 The reference list

[1] TATIČ, M., LUKÁČ L.: *Industrial kilns I*, TUKE 2009.

[2] *Crushing technology* - Available online: *https://www.kleemann.info/en/technologies/crushing-technology/* [20 Februar 2018].

[3] ANDRITZ Pulp &Paper – *Kiln ringing* – company literature 2009.

[4] LANGOIS, J.: *Ash ring – fuel and specification*, National lime association, 2002.

[5] ALSOP, A. P: . *Cement plant operations handbook*, Surrey, 1998

Advances in Thermal Processes and Energy Transformation
Volume I, 2018, Bory01, p.05-09
ISSN 2585-9102

Measurement Errors in Research of Adhesion f Scale to the Steel substrates

Jarosław Boryca [1] ● Tomasz Wyleciał [1] ● Dariusz Urbaniak [2]

[1]Faculty of Production Engineering and Materials Technology, , Czestochowa University of Technology, Al. Armii Krajowej 19, 42-200 Częstochowa, Poland, contact meil: jboryca@op.pl
[2]Faculty of Mechanical Engineering and Computer Science, Czestochowa University of Technology, Al. Armii Krajowej 21, 42-200 Częstochowa, Poland,

Category : Original Scientific Paper,
Received : 02 February 2018 / Revised: 24 Februeary 2018 / Accepted: 07 Marec 2018

Keywords : Measerement errors, Adhesion, Steel

Abstract : The article presents the research methodology and the position for measuring the adhesion of scale. The results of the research are presented and the analysis concerning the calculation of measurement errors during measurements of adhesion of scale to the steel substrate is presented.

Citation: Boryca, J., et al.: Measurement Errors in Research of Adhesion f Scale to the Steel substrate, Advance in Thermal Processes and Energy Transformation Volume 1,Nr 1 (2018), p. 05-09, ISSN 2585-9102

1 Introduction

The processes of heating steel charge before plastic working are inseparably accompanied by steel oxidation. As a result of this phenomenon, scale forms, whose presence poses a substantial problem both for the heating process and for the subsequent plastic working.

For a long time, the world's metallurgy has been pursuing the goal of reducing the heat consumption. An important issue related to this objective is the reduction of the amount of forming scale by selecting an appropriate heating technology. This problem has been widely covered in publications [1÷4].

Heating of charge before plastic working is done primarily in pusher and stepper furnaces that are continuous operation furnaces. Each shutdown of the operation of such a unit results in heat losses. These shutdowns are largely caused by the necessity of carrying out repairs and overhauls of furnace hearths that have been damaged by the action of scale falling down during heating. This constitutes a major problem for the manufacturers of both metal sheets and plates and sections.

After exiting the furnace and prior to rolling, the steel surface should be cleared of scale. However, if the adhesion of the scale is too high, it will not be wholly removed. As a consequence, laps will form in the plastic working process, whose removal will require a laborious and costly treatment. This, however, impairs the quality of products [5]. The problem of too high scale adhesion occurs also in the wire drawing process. Indeed, scale residues left on the wire rod are pressed into the material during wire drawing and give rise to an intensive wear of the drawing dies [6].

Thus, it can be concluded that the next stage in the improvement of the heating process should be developing a technology that minimizes steel loss, but, at the same time, guarantees such scale adhesion to the steel substrate that the scale will not come off the steel surface in the furnace and allow itself to be removed after leaving the furnace.

2 Measuring stand and research methodology

To realize the objective of the research, a specialized laboratory has been built at the KPPiOŚ (Department of Industrial Furnaces and Environmental Protection). The basic element of the measuring stand is an electric furnace, type KS 520. A combustion chamber with a gas burner are integrated with the furnace. The burner performs the role of a gaseous atmosphere generator. The temperature in the furnace is controlled by means of a TROL – 9090 regulator. The accuracy of temperature control is ±1.0K. In order to determine the adhesion of scale for mass method, a scale knocking-off device was designed and constructed. A set of

measuring testing stands discuss in work more widely [7÷9].
It was assumed that the degree of specimen surface cleaning after partial chipping off of the scale layer would be essential for the measurement. The mass method of determining the adhesion of scale involves the weighting of samples in the successive stages of the research. The adhesion of a scale layer can be expressed by the ratio of the mass of scale left after knocking off to the entire mass of the scale. The value of so determined adhesion is defined by the following equation [10]:

$$P = \frac{m_2 - m_3}{m_1 - m_3} \cdot 100\% \qquad (1)$$

where:
m1 – mass of the sample after heating, kg,
m2 – mass of the sample after scale knocking off, kg,
m3 – mass of the sample after complete cleaning, kg,
P – adhesion of scale, defined by the percentage fraction of scale left on the steel core after hitting by the ram, %.
The masses m2 and m3 are determined by weighting the sample. For the determination of the mass m1, the following equation is used:

$$m_1 = m_0 + \frac{z \cdot A}{0{,}74} \qquad (2)$$

where:
m0 – mass of the sample before heating, kg,
z – loss of steel for scale, kg/m2,
A – sample surface area, m2.

For the determination of the loss of steel, the following p equation is used:

$$z = \frac{m_0 - m_3}{A} \qquad (3)$$

Scheme of course of research with utilization of the mass method is shown in Fig. 1

3 Results of adhesion measurements

It carry measurements of masses of samples in the successive stages of the test. Calculation of the loss of steel and scale adhesion on the base of carried measurements was executed. The heating were varied out with the value of combustion air excess ratio of □=0.6□1.4. and heated in temperature 900, 1000, 1100, 1200 and 1300°C. Results of measurements and accounts summarized in Table 1 and Table 2.

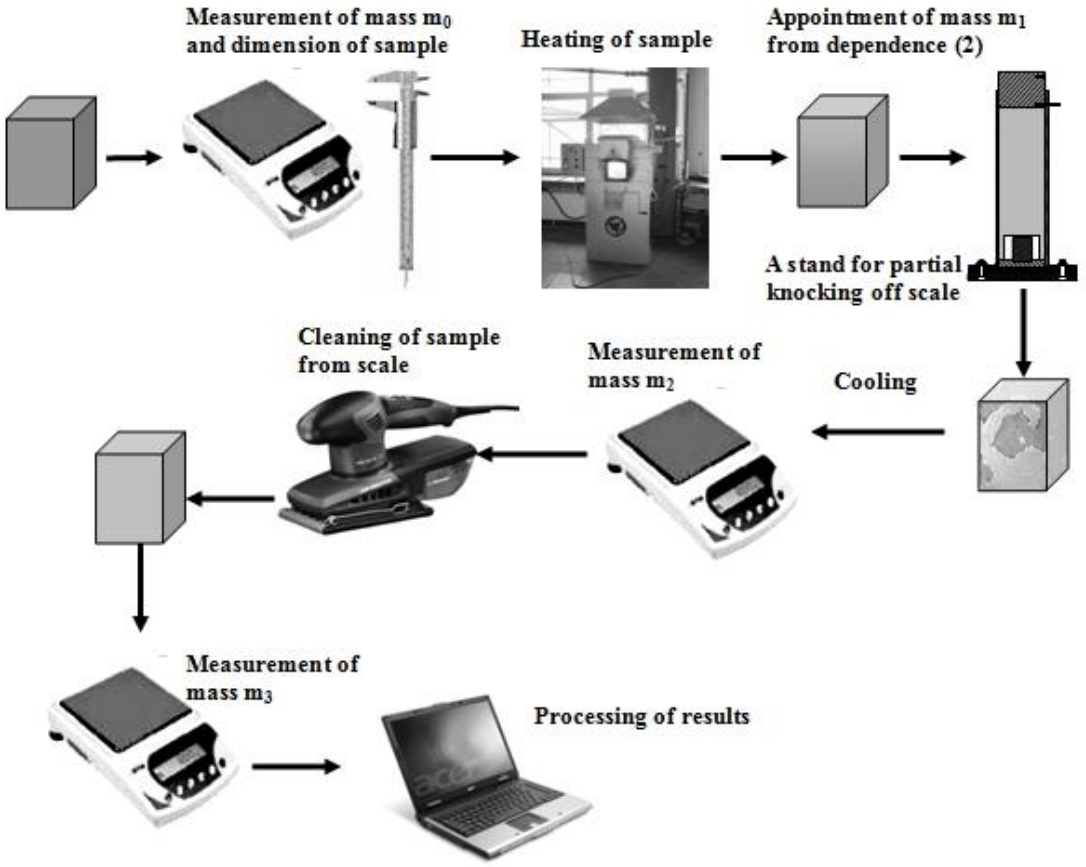

Figure 1 Scheme of course of research with utilization of the mass method [11]

Table 1 The results of the measurements of sample masses and steel losses for scale and scale adhesion for α≤1.0

α	t, ˚C	m_0, g	m_1, g	m_2, g	m_3, g	z, kg/m^2	P, %
0.6	900	349.877	355.769	350.175	349.459	0.545	11.35
	1000	349.917	360.328	350.403	348.517	0.963	15.97
	1100	349.610	366.551	349.660	345.371	1.567	20.25
	1200	350.905	376.700	349.428	338.542	2.386	28.53
	1300	349.620	386.842	347.784	327.984	3.443	33.64
	1330	350.159	391.337	345.018	319.624	3.809	35.41
0.7	900	351.786	358.771	351.766	350.973	0.646	10.41
	1000	349.489	361.488	350.944	349.214	1.142	14.06
	1100	349.524	368.378	350.769	346.741	1.857	18.02
	1200	350.714	380.487	350.586	340.762	2.826	24.72
	1300	349.424	392.248	341.053	318.903	4.079	30.13
	1330	349.486	397.055	333.721	304.271	4.513	31.74
0.8	900	349.522	357.412	349.043	348.123	0.748	9.91
	1000	349.217	363.152	349.695	347.823	1.322	12.21
	1100	352.452	375.114	349.033	344.293	2.150	15.38
	1200	349.671	384.181	350.327	342.376	3.274	19.02
	1300	349.850	399.643	353.651	338.426	4.724	24.87
	1330	350.347	405.442	354.043	335.682	5.227	26.32
0.9	900	349.974	359.185	341.784	340.027	0.852	9.17
	1000	349.786	366.056	342.470	339.588	1.505	10.89
	1100	351.150	377.615	342.596	337.474	2.448	12.76
	1200	349.961	390.242	344.219	335.032	3.726	16.64
	1300	350.728	408.869	348.424	332.752	5.378	20.59
	1330	350.387	414.711	348.641	328.817	5.950	23.08
1.0	900	350.387	414.711	348.641	328.817	0.956	7.86
	1000	350.793	361.128	334.829	332.586	1.690	9.32
	1100	350.412	368.682	335.303	331.872	2.749	11.74
	1200	349.922	379.641	336.042	330.243	4.184	14.67
	1300	349.829	395.061	338.830	329.163	6.038	17.71
	1330	349.445	414.721	341.508	325.752	6.682	18.93

Table 2 The results of the measurements of sample masses and steel losses for scale and scale adhesion for α>1.0

α	t, ˚C	m_0, g	m_1, g	m_2, g	m_3, g	z, kg/m^2	P, %
1.1	900	350.274	362.004	325.863	323.593	1.085	5.91
	1000	349.875	369.270	328.993	325.906	1.794	7.12
	1100	350.144	379.928	332.535	328.008	2.755	8.72
	1200	349.893	393.039	339.298	332.966	3.991	10.54
	1300	349.251	408.894	346.641	336.279	5.517	14.27
	1330	349.884	415.095	352.761	340.658	6.032	16.26
1.2	900	348.808	361.129	318.615	317.247	1.169	3.12
	1000	349.761	370.115	321.823	318.951	1.931	5.61
	1100	349.259	380.522	324.271	320.115	2.966	6.88
	1200	348.115	394.418	329.586	323.130	4.298	9.06
	1300	348.861	411.482	338.781	327.452	5.941	13.48
	1330	349.973	418.434	345.059	331.679	6.495	15.42
1.3	900	350.365	363.889	312.430	311.127	1.251	2.47
	1000	349.685	372.031	314.597	312.483	2.067	3.55

	1100	349.824	384.148	317.331	314.094	3.175	4.62
	1200	350.258	399.988	321.482	315.673	4.600	6.89
	1300	349.318	418.064	327.522	318.491	6.359	9.07
	1330	349.914	425.071	334.450	321.052	6.952	12.88
1.4	**900**	348.839	362.825	305.427	304.726	1.332	1.21
	1000	349.327	372.496	306.224	305.117	2.202	1.64
	1100	348.104	382.426	307.676	305.931	3.381	2.28
	1200	348.452	397.914	309.993	306.672	4.899	3.64
	1300	349.580	420.817	314.591	308.215	6.772	5.66
	1330	349.607	427.909	319.964	310.729	7.404	7.88

4 Analysis of measurement errors

Due to many reasons, which have a source in the imperfection of the measuring apparatus, observation imperfections and the elusive influence of the environment, each physical value determined by measuring and expressed in a particular number is different from the actual value of that quantity. The difference between the measurement value and the actual value is called an absolute error. The relative standard error of measurement is equal to the ratio of the absolute error to the actual value [12].

Several reasons can affect the magnitude of measurement error. Systematic and accidental errors are distinguished depending on the type of cause and nature of the error [12÷18]. Systematic errors always have the same effect on the measurement result made using the same measuring apparatus and measurement method. Accidental errors are the result of many minor and variable factors of accidental causes.

In the paper in the presented research, the cause of systematic errors can be:

- measurements of dimensions sample, ±10-5 m,
- measurements of the mass of samples before and after heating, ±10-6 kg,
- measurements of the heating time, ±10 s,
- accuracy of the temperature control, ±1K,
- accuracy of regulation of gas and air flow, ±10-2 m3/h.

To calculate ΔP, for the scale adhesion determined by the mass method, the equation (1) should be written in the form:

$$P = \left(\frac{m_2}{m_1 - m_3} - \frac{m_3}{m_1 - m_3} \right) \cdot 100\% \quad (4)$$

and then perform calculations using the absolute differential method [18] separating equation (4) into two parts:

$$\Delta P = \left(\Delta P_1 - \Delta P_2 \right) \cdot 100\% \quad (5)$$

Hence the:

$$\Delta P_1 = \left| \frac{\partial P_1}{\partial m_2} \right| \cdot \left| \Delta m_2 \right| + \left| \frac{\partial P_1}{\partial m_3} \right| \cdot \left| \Delta m_3 \right| + \left| \frac{\partial P_1}{\partial m_1} \right| \cdot \left| \Delta m_1 \right| \quad (6)$$

And

$$\Delta P_2 = \left| \frac{\partial P_2}{\partial m_3} \right| \cdot \left| \Delta m_3 \right| + \left| \frac{\partial P_2}{\partial m_1} \right| \cdot \left| \Delta m_1 \right| \quad (7)$$

where:

Δm2= Δm3=10-6 [kg].

The value of Δm1 was calculated method of the absolute differential on the basis of the formula (2):

$$\Delta m_1 = \left| \frac{\partial m_1}{\partial m_0} \right| \cdot \left| \Delta m_0 \right| + \left| \frac{\partial m_1}{\partial z} \right| \cdot \left| \Delta z \right| + \left| \frac{\partial m_1}{\partial A} \right| \cdot \left| \Delta A \right| \quad (8)$$

where:

Δm0=10-6kg.

Detailed calculations of Δz values are presented in the paper [19]. Based on the dependencies presented there, calculations were made and a result was obtained $\Delta z = 0.00470$ kg/m2.

The value of ΔF was calculated by means of the absolute differential method from the dependence on the surface of the cuboid:

$$\Delta A = \left| \frac{\partial A}{\partial a} \right| \cdot \left| \Delta a \right| + \left| \frac{\partial A}{\partial h} \right| \cdot \left| \Delta h \right| \quad (9)$$

After differentiation dependence was obtained:

$$\Delta A = 4 \cdot (a + h) \cdot \left| \Delta a \right| + 4a \cdot \left| \Delta h \right| = \pm 4.4 \cdot 10^{-6}, \, m^2 \quad (10)$$

Differentiating and substituting the results of calculations to dependence (8) it was obtained:

$$\Delta m_1 = 1 \cdot \left| \Delta m_0 \right| + A \cdot \left| \Delta z \right| + z \cdot \left| \Delta A \right| = 4.1 \cdot 10^{-5}, \text{ kg.} \quad (11)$$

Differentiating and substituting the results of calculations to dependencies (6) and (7) it was obtained:

$$\Delta P_1 = \frac{1}{m_1 - m_3} \cdot |\Delta m_2| + \left(- \frac{m_2}{(m_1 - m_3)^2} \right) \cdot |\Delta m_3| + \left(- \frac{m_2}{(m_1 - m_3)^2} \right) \cdot |\Delta m_1| \quad (12)$$

$$\Delta P_1 = -9464 \cdot 10^{-6}, \ \%,$$

And

$$\Delta P_2 = \frac{m_1}{(m_1 - m_3)^2} \cdot |\Delta m_3| + \left(- \frac{m_3}{(m_1 - m_3)^2} \right) \cdot |\Delta m_1| \quad (13)$$

$$\Delta P_2 = -8660 \cdot 10^{-6}, \ \%.$$

Substituting for formula (5), the value of the absolute statistical error for the adhesion measure was obtained $\Delta P = \pm 0.8$ %.

The average value of the adhesion measure will be:

$$\overline{P} = \frac{\sum_{i=1}^{n} P}{n} = \frac{733.48}{48} = 15.28, \% \quad (14)$$

The average value of a relative systematic error is:

$$\delta = \frac{\Delta P}{\overline{P}} \cdot 100\% = 0.052 \ , \% \ (15)$$

5 Summary

In measuring the scale adhesion indirect and direct measurement errors and calculation inaccuracies may occur. Based on the calculated values of measurement errors, it can be concluded that the measurement of the adhesion of the scale to the steel substrate has been carried out with high accuracy.

The accuracy of measurements can also be affected by accidental errors to which, in the case of the presented research, can be included:

- changes in ambient parameters,
- fluctuations in the chemical composition of the gas,
- accuracy of descaling from the surface of samples,
- fluctuations in gas pressure,
- fluctuations in air pressure,
- other.

6 The reference list

[1] NEUMANN F. : Metallurgische Betrachtungen zum Oxydationsverhalten von Stahl bein Erwarmen, Harterei-Tech., pp. 198-207. 1971.

[2] WAWRZYK P., WESSELY P., Bezzgorzelinowe nagrzewanie stali w piecach grzewczych, „Śląsk", Katowice 1973.

[3] SZARGUT J., KOZIOŁ J., MAJZA E., Zasady poprawy eksploatacji pieców grzejnych, *Zeszyty Naukowe Pol.*, Energetyka z. 106., Gliwice 1989.

[4] KIELOCH M.: Energooszczędne i małozgorzelinowe nagrzewanie wsadu stalowego, Metalurgia nr 29, Częstochowa 2002.

[5] HIGGINSON R. L., et all.: Texture development in oxide scales on steel substrates, Scripta Materialia 2002, nr 47, s. 337-342.

[6] GOLIS B., et all.: Druty stalowe, Politechnika Częstochowska, Metalurgia nr 35, Częstochowa 1991.

[7] BORYCA J., Przyczepność warstwy zgorzeliny powstałej w procesie nagrzewania wsadu stalowego, Doctoral work, Częstochowa 2005.

[8] BORYCA J., et all.: Investigation of the adhesion of scale forming in the process of steel charge heating before plastic working, *Archives of Metallurgy and Materials*, Vol.51, nr 3, 2006.

[9] KIELOCH M., et all.: Przyczepność zgorzeliny w procesie nagrzewania wsadu stalowego, *Hutnik*, nr 1, pp. 7-12. 2005.

[10] BORYCA J., et all.: The Effect of Condition of the Charge Surface on the Scale Adhesion for Excess Air Combustion, *Metalurgija*, Vol.54, 2015.

[11] BORYCA J., et all.: Analysis of influence of heating time on the scale adhesion to the steel surface, *Acta Metallurgica Slovaka*, Vol. 13, 2017.

[12] KOTLEWSKI F.: Pomiary w technice cieplnej, WNT, Warszawa 1972.

[13] KULESZA J.: Pomiary cieplne, WNT, Warszawa 1993.

[14] RYSZKA E., Pomiary zapylenia gazów w przewodach, „Śląsk", Katowice 1972.

[15] STRZAŁKOWSKI A., ŚLIŻYŃSKI A.: Matematyczne metody opracowywania wyników pomiarów, PWN, Warszawa 1969.

[16] MICHAŁOWSKI M., et all.: Badania i pomiary cieplne pieców w hutnictwie żelaza, „Śląsk", Katowice 1973.

[17] HANSEL H., Podstawy rachunku błędów, WNT, Warszawa 1968.

[18] ROMANOWSKI Ś., WRONA W., Matematyka wyższa dla studiów technicznych - część I. PWN, 1967.

[19] KIELOCH M.: Strata stali w piecach grzewczych przy zmiennej temperaturze nagrzewania, nr 22, Częstochowa 1991.

Review process

Single-blind peer reviewed process by two reviewers

Advances in Thermal Processes and Energy Transformation
Volume I, 2018, Flim01, p. 10-13
ISSN 2585-9102

Application of infrared method for thermal comfort workplace evaluation

Marián Flimel[1]

[1] *Department of Process Technique, Technical University of Košice, Faculty of Manufacturing Technologies with a seat in Prešov, Bayerova 1, 080 01 Prešov, Slovak Republic, marian.flimel@tuke.sk*

Category : Original Scientific Paper,
Received : 10 February 2018 / Revised: 03 Marec 2018 / Accepted: 20 Marec 2018

Keywords : infrared method, temperature, Thermovision

Abstract : Thermal comfort as a state of physical and mental well-being in a given environment is an important factor in maintaining the health, satisfaction and performance of a person. There are several methods to evaluate it. The subject of this article is the possibility of using an infrared method for determining cumulative room temperature and the temperature difference between the air temperature and the surface temperature of the room construction. There is an example given for the application.

Citation: Flimel Marián: Application of infrared method for thermal comfort workplace evaluation, Advance in Thermal Processes and Energy Transformation, Volume I, Nr. 1(2018), p. 10-13, ISSN 2585-9102

1 Introduction

Thermal comfort and thermal discomfort are two diametrically opposed conditions, which one feels in the internal (external) environment of buildings. [1][2]. Table 1 shows the human interaction with thermal environment in two positions of perception – thermal comfort and thermal discomfort.

Table 1 Interaction of person with thermal environment – their elements [3]

Thermal comfort = balance between person and environment should be ensured by :	Thermal discomfort – discomfort creates:
Indoor temperature θ_{ai} or Exterior temperature θ_{ae}	Heat radiation asymmetry
Medium radiation temperature θ_r	Excessive temperature gradient of air
Air flow velocity v_a	Drafts, air flow
Air velocity v_a	Draught, air flow
Isolation of human clothing I_{cl}	Too hot or cold floor
Resistance of clothing against the evaporation of sweat R_{cl}	Too hot or cold ceiling
Human metabolism M	
Occupation – activity W	

The evaluation of measured value (from the first column in Table 1) is based on the heat balance factors which are acting between human and thermal environment – internal production of heat (M), heat transfer by radiation (R), heat conduction (C), evaporation (skin –E, respiration – Eres) and flowing – respiration (Cres).

2 Cumulative room temperature evaluation

Cumulative room temperature θM is one of the qualitative indicators for assessing internal environment of buildings in relation to the thermal comfort. The theoretical calculation of the cumulative temperature for heating or summer season is known. Assessing the value under in situ conditions is possible in operating mode of an empty room or with the inhabitants using the appropriate measurement devices. Determining the mean surface temperature of constructions bounding the room appears to be a tough problem. Therefore an infra-red method for assessing the mean surface temperature of a surface has been chosen. The paper describes the combined method application procedure (air temperature measurement method + infra-red method – thermography), as well as an example of its application.

It is possible to identify thermal comfort of building's users using Cumulative room temperature θM described by the following equations [1]:

$$\theta_M = \theta_{ai} + \theta_s \quad (1)$$

$$\theta s = (\theta_{si1}.A_1 + \theta_{si2}.A_2 + ... \theta_{sin}.A_n):(A_1+A_2+ ....+A_n) \quad (2)$$

where:
θ_M is cumulative room temperature, (°C),
θ_{ai} is indoor air temperature (°C),
θ_s is average surface temperature of the surrounding areas , mean radiation temperature (°C),
θ_{si1}, θ_{si2}.. θ_{sin} are temperatures of inner surfaces of building structure (°C),
A_1, A_2,....A_n are the surfaces of individual structures (m2).

Residential and civic buildings are required to meet a winter condition for $\theta_M \geq 38$ °C and summer condition for $\theta_M \geq 51$ °C while the air speed is maximum 0,1 m/s, relative humidity between 35 – 50%, including additional condition that $\theta_{ai} \leq 27$ °C, $\theta si \leq 27$ °C. In the design stage of a building construction plan it is possible to calculate and assess θ_M on the base of standardized thermo-technical values and boundary conditions. The indoor air temperature and average surface temperatures of building structures under in situ conditions have often uneven progress thanks to permanent service within the room. Therefore the current calculation of θ_M in this situation would be inaccurate. Proposed infrared method (thermography) for determining the average surface temperature θ_s replenishes the classic air temperature measurement θai and the assessment of θ_M.

3 Determination procedure of cumulative room temperature under in situ conditions

Assessment of room thermal comfort using the cumulative room temperature under in situ conditions is possible using two methods:

a) Determination of air temperature θ_{ai} (°C) (dry temperature) or simply determining the temperature nearby human body or any human not affected by temperature radiation of any surrounding areas. Temperature is measured by thermometers in close distance from a person. If the working position in not known then we measure 1,5 m far from the floor.

b) To determine the average surface temperature of the surrounding areas (walls, windows, ceiling, floor), variety of temperature sensors to measure the surface temperatures can be used. Using these sensors (contact or contactless thermometers) we will obtain only local temperature values. In order to get the average surface temperature of the whole area, we need much more measurements, so that the measuring point net becomes more dense and the result of the average surface temperature becomes more accurate. This kind of measurement is time consuming and the surface temperatures tend to change over the measurement period. It is essential to apply the Thermal imaging measurements which is able to display the surface temperatures of the whole area at once. Depending on the type of thermal imager (the software equipment) the below mentioned procedure is applicable.

This the procedure of determination of average surface temperature of the building structure by applying thermo imager (for case assessment on window construction) respecting the boundary conditions suitable for measurement.

1. Set the required parameter of imager (MOBIR M4 – date of measurement, time, room humidity, distance, predominant material emissivity).
2. Specify the construction to be evaluated and perform the thermo image, then set parameter for another construction. For constructions of large dimensions divide the surface into smaller fragments which can be captured by camera lens.
3. Evaluate the corresponding image by computer software.
4. Determine the assessment area as an intersection of two rectangles (polygons) using the appropriate software, as in Fig. 1 and Fig. 2.
5. Enter the appropriate values of surface temperatures into table, then evaluate the next part of the construction.
6. Each view of the thermal imager is assigned a real area determined from the construction dimensions of certain room.
7. Appropriate values can be calculated right in the table (effectively in Excel format).

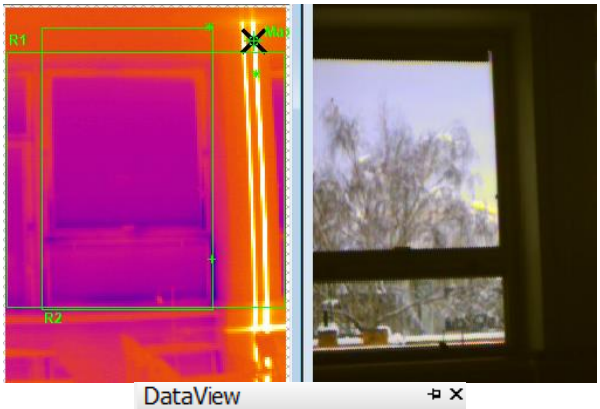

DataView

Obj…	Te…	Property
Max	55.7…	Tempera…
R1	56.5…	MaxTemp
	18.2…	AvgTemp
	5.8°C	MinTemp
R2	23.5…	MaxTemp
	16.2…	AvgTemp
	5.8°C	MinTemp

Figure 1 Thermovision image, intersection of two rectangles R1 and R2 with assesed teperatures in table

The advantages of the presented method for determination of cumulative room temperature can be:

- Assesing speed of the values in given time,
- Accuracy of the assessed surface temperatures due to the area under consideration,

• Determination of surface temperatures on the interior elements, e.g. walls, furniture, radiators, which is a disadvantage at the same time when preventing us from measurment of building structure temperature.

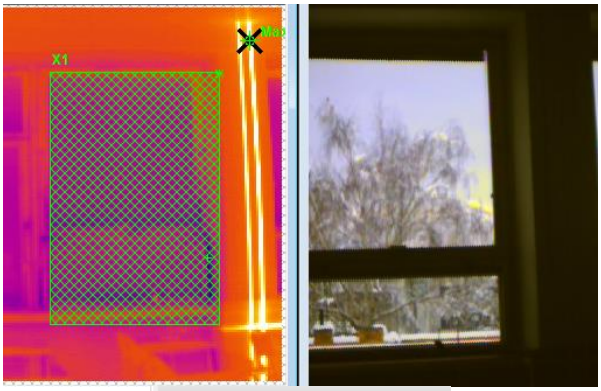

Figure 2 Surface X1 determining the average surface temperature of the whole window

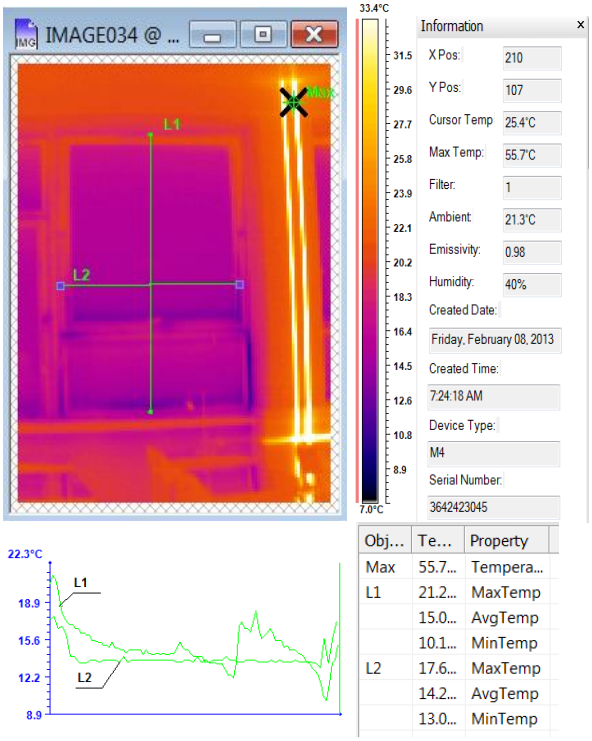

Figure 3 Course of the surface temperature through the window in linear investigation on section lines L1, L2

The disadvantages (constraints) of infra red method may be:

• Entry of a single material emmisivity even if there are more than one material,

• Limited using conditions in winter (temperature difference must be higher than 15°C .

• Measuring the mean radiant temperature Vernon-Jokl thermometer is a time faster than time losses in the formation of various thermography of surfaces .

The assessor, evaluator plays an important role in while measurement. He or she can also be the source of error if s/he is not skilled in measurement methodics, not to mention the possible inaccuracy of measurement devices. Outputs from measurement of the average surface temperatures have been entered into Tab. 1, subsequently we can calculate the summary room temperature for office with dimensions 3m x 6,0m x 2,9m and for heating season.

Table 2 Exemplary calculation of Cumulative room temperature

construction	determine the surface temperature construction - θ_{si} (°C)	area – A_i (m^2)	$\theta_s . A_i$ (°C. m^2)
1. floor	20,1	18,0	361,8
2. ceiling	21,1	18,0	379,8
3. inside wall	20,3	17,4	353,2
4. inside wall without door	20,0	7,1	142,0
5. door	19,8	1,6	31,68
6. external wall	18,2	17,4	316,68
7. external wall without window	18,0	3,66	65,88
8. window (from fig.2)	15,4	5,04	77,61
the sum of columns		88,2	1728,65
the average surface temperature of the surrounding areas - θ_s		1728,65 : 88,2 = 19,59	
indoor air temperature - θ_{si}		20,5 °C	
cumulative room temperature- θ_M		20,5 + 19,56 = 40,09°C	

We see that θ_M = 40.09 ° C ≥ 38.0 ° C, which is satisfactory; the difference of air temperatures – surface radiation asymmetry on window construction Δθ = 20.5 - 15.04 = 5.46 ° C ≤ 10 ° C is satisfactory.

Figure 4 Course of surface temperatures in the corner of peripheral case (outdoor temperature of air +2°C)[5]

Application of the previous thermal images(Fig.4) is possible during the elimination of thermal bridges because there is a risk of mould formation.

4 Summary

The importance of application of the above described methodology for determining the cumulative room temperature lies in its flexibility and ability to react quickly to rapidly changing conditions. It is possible to

record temperature changes in the interior (due to heating sources, sunlit, heat flows from the technology, etc.) and to evaluate them. Whether we feel cold or hot from surrounding structures depends on the temperature difference ($\Delta\theta = \theta ai - \theta si$) and the distance from the structure . People rotate often over different work positions within the work environment which results in changes in cumulative temperature of the room. The infra red method determines the thermal contribution of each structure for assessment of average temperature of surrounding area and determines the most significant construction. At the same time the inequalities are diagnosed – inhomogeneous structures and thermal bridges, which give rise to subjective mentioned "feeling cold" and heat in room, respectively . The benefit of the described method is also the visualization (infrared photography of surfaces) indoor environment . The application of infrared method is important during the determination of qualitative and quantitative material properties in diagnostic processes, building construction, thermal comfort and devices by non-destructive method.

5 The reference list

[1] MACPHERSON, R. K.: Thermal Stress and Thermal Comfort, *Ergonomics*, vol. 16, pp. 611- 622, 2007.

[2] SASAMOTO, T., et al.: Control of indoor thermal environment based on concept of contribution ratio of indoor climate. *Building Simulation*, vol. 3, pp. 263-278, 2010.

[3] STN EN ISO 7726, Ergonomics of the thermal environment - Instruments for measuring physical quantities, 2003.

[4] FLIMEL, M.: Determining cumulative room temperature under in situ conditions using combined method, *Advanced Materials Research* : Envibuild 2013, Vol.899 pp. 116 – 119, 2014.

[5] FLIMEL. M., DUPLÁKOVÁ, D.: Application of infrared spectrometry in the diagnostic process in situ, *International Journal of Interdisciplinarity in Theory and Practice*. No 12, pp.35-39, 2017.

Review process

Single-blind peer reviewed process by two reviewers.

Advances in Thermal Processes and Energy Transformation
Volume I, 2018, Kara01, p.14-18
ISSN 2585-9102

Basic areas of the secondary energy resources use in the blast-furnace ironmaking and application of heat pumps for utilization of sensible heat of the furnace top gas

Yevgeniy Karakash[1]

[1] *The department of Ecology, Heat-Transfer and labour protection, Faculty of Mechanical Engineering, NMetAU, av. Gagarina, 4, Dnepropetrovsk, 49600, Ukraine, e-mail: yevgenkarakash@gmail.com*

Category : (Short communication, Original Scientific Paper, Preliminary Communication, Review Article, Professional Paper, Technical Note, Application)
Received : 10 Februar 2018 / Revised: 08 March 2018 / Accepted: 21 March 2018

Keywords: blast-furnace, combustion, energy consumption, heat pump, ironmaking

Abstract: Reduction of specific energy consumption at cast-iron production is the topical issue over several decades. One of basic areas of the specific energy consumption reduction is the specific coke consumption reduction due to injection of pulverized coal fuel (PCF). Under the present-day conditions of blast-furnace shop operation, the use of low-potential SERs seems to be the most promising measure with regard to reduction of cast-iron production cost. Proposed measures on improvement of blast-furnace gas calorific power due to the reduction of its moisture content allow the blast-furnace air temperature increase and coke consumption reduction. Also proposed is partial transfer of excess heat from the blast-furnace gas to combustion air by means of the system of heat pumps, which allows increase in calorimetric combustion temperature. In this paper, main parameters are calculated of the heat pump system operation under the conditions of blast-furnace shop at the increased top gas temperature. This paper presents heat pump system operating efficiency and determines conversion factor for the specific conditions (COP).

Citation: Karakash Y.: Basic areas of the secondary energy resources use in the blast-furnace ironmaking and application of heat pumps for utilization of sensible heat of the furnace top gas, Advance in Thermal Processes and Energy Transformation Volume I, Nr. 1(2018), p. 14-18, ISSN 2585-9102

1 Introduction

For what concerns the energy consumption by modern metal manufacturers in Ukraine, its structure is approximately as follows:

1) Coke – 32-35%;
2) Natural gas – 13-16%
3) Blast-furnace gas – 17-20%
4) Coke oven gas – 7-9%
5) Power-generating coal – 2-4%
6) Heavy fuel oil – 2-4%
7) Other fuel types – up to 1%
8) Electric power – 15-20%

Energy consumption pattern broken down by main process areas of the metallurgical industry in 2010-2016 is as follows: sintering process – 6-8% of total industry-consumed energy; coking process – 4,5-6%; blast-furnace ironmaking – 47-50%; steelmaking – 6-11% (at this processing stage, number of electric furnaces increases sharply); rolling process – 6-9%; refractory production – 1-2%; electric power installations – 12-14%; other consumers – up to 7%.

Coefficient of major SERs utilization does not exceed 40%, which indicates low efficiency of recuperation plants and systems. Since blast-furnace processing is one of primary energy consumers in the industry, improvement of its operating efficiency and introduction of new energy-saving technologies would allow considerable reduction in total industry-wide power costs.

Pulverized coal injection technology is used in growing number of blast furnaces.

Depending on the used technology and PCF quality, this measure provides coke consumption savings of 40% to 10%. Previously, coke consumption for cast-iron production made 500-550 kg per ton of cast-iron, and now some plants reduced this value to 270-237 kg of coke per ton of cast-iron due to the use of PCF.

However, number of processing complexities is related to the PCF preparation process. Primarily, this

is proper drying prior to injection into furnace through air tuyeres. Natural and blast-furnace gases can be used for drying, as well as combustion products escaping from hot-blast stove being the secondary energy resource (SER), of which efficient use would result in the cast-iron production cost reduction. It might be well to evaluate the SER use at the blast furnaces in present-day conditions.

2 Performance potential of blast-furnace complex constituents with regard to the SER usage

Major portion of total thermal energy generated in furnace shaft and carried in with the hot air blast is lost:

1) *Blast furnace;*
2) *Blast furnace gas treatment system;*
3) *Hot stoves.*

1) Blast furnace - for the physical and chemical processes inside furnace shaft, for the change of enthalpy and melting of charge components, for the finished cast-iron and slag overheat, and for heating the heat-transfer medium and change of its aggregate state in the cooling system; in addition, part of thermal energy is carried off with the furnace top gas.

The most practicable SER sources are sensible heat of cooling system heat-transfer medium, sensible heat of top gas and partial usage of the overheated liquid slag heat. However, such SER usage is scarcely adopted, except for the occasional use of heat-recovery boilers in the evaporation cooling systems [2]. The use of sensible heat of overheated liquid cast-iron is challenging target even in theoretical terms, because its overheating is relatively low.

In the blast furnace cooling systems, water is the basic heat-transfer medium; in the evaporation cooling systems, it may exist both in gaseous and liquid states. At the most enterprises, water is cooled with the use of cooling towers or special cooling ponds without sensible heat utilization.

2) Blast furnace gas treatment system.

Sensible heat of furnace top gas is main and sole heat resource at this facility. When leaving the blast furnace, top gas temperature ranges from 170°C to 450°C depending on blast-furnace smelting features. While cleaned blast - furnace gas temperature makes from 15°C to 65° C, respectively. The use of high temperature of top gas in conventional heat exchangers upstream the gas treatment system is complicated due to considerable dust content (up to 20g/m^3). Conventional heat exchangers are virtually inoperative at such dust content in one of heat-transfer media.

3) Hot-blast stoves.

Main secondary thermal energy source is chimney gas with temperature 180-250° C from hot-blast stoves [3]. These SERs are successfully used at many enterprises; however, there is number of limitations as well, which reduce sensible heat utilization efficiency. These include minimum temperature condition for fumes from heat exchanger; temperature must be higher than or equal to 110-230° C, since it is the level of dew point of sulphuric acids contained in fumes. When fume temperature drops below the indicated value, condensed moisture is deposited on the heat exchanger walls resulting in the acid corrosion. Such phenomena cases were observed at the Zaporizhstal Iron & Steel Works in 2005.

Thus, it may be concluded that SER are only partly used in the most example cases [4].

2.1 The use of the system of heat pumps and their calculation for the blast-furnace shop conditions

The study proposes the use of the sensible heat utilization system based on heat pumps and heat transfer tubes. This system includes intermediate heat-transfer medium and is capable of operation with low-grade sources of sensible heat [5].

One of proposed solutions for the set problem is extraction of energy from the blast-furnace gas, both upstream and downstream the gas treatment system. Here, heat exchanger with intermediate heat-transfer medium (Freon or oil) has not necessarily contact directly with the dust-carrying top gas, but can be securely attached to the external surface of top gas discharge duct. In this case, heat amount taken from the top gas would depend on the heat-exchange surface area, aggregate coefficients of heat transmission from surface to the gaseous medium at the “hot” and “cold” sides, and on the heat-transfer resistance in the points of tubing contact with the top gas line surface. On the average, furnace top gas temperature could be decreased by 70-120°C prior to the entry into gas treatment system. Alternatively, heat exchanger with intermediate heat-transfer medium could be installed inside the air duct supplying combustion air into hot-blast stoves (HS). Such installation efficiency could make 45-80%, which allows hot blast temperature increase by 10-15°C. At the total reduction in blast-furnace gas consumption for HS heating by 6-8%, average value of savings on specific energy consumption in the blast-furnace processing would make approximately 0.5% [6]. When engineering the proposed system, installation of compressor equipment and expansion valves (included in every heat pump system) could be eliminated, as well as the change of aggregate state of intermediate heat-transfer medium. Completed system is the system of heat exchangers with intermediate high-temperature heat-transfer medium. However, if temperature at the “hot” side of such system is below 180-200°C, such equipment

modification seems being of little promise. Moreover, the use of classic heat pump or heat transfer tubes is only practical for the blast-furnace gas temperature downstream the gas treatment system. Gas temperature downstream the gas treatment system makes 40-65°C. It should be noted that heat utilization at lower temperatures is quite impractical. In our opinion, primary objective in this case is not so much utilization of small amount of sensible heat as total blast-furnace gas temperature reduction downstream the burners. The matter is that the blast-furnace gas with relatively high temperature (45°C and over) has sufficiently high moisture content, which reduces its calorific heat value. The work [6] considers in some detail the blast-furnace gas moisture content data from existing furnaces versus temperature and impact of these parameters on the eventual combustion temperature in HS. The use of heat pump with Freon-type heat-transfer medium in the internal circuit is proposed for this heat utilization and blast-furnace gas temperature reduction.

Following is calculation of such heat pump system for operation with low-grade thermal energy source under the blast-furnace shop conditions.

2.2 Calculation of heat pump performance

Calculation of evaporator for blast-furnace gas cooling

Input data:

Refrigerating fluid – Freon R22.

Refrigerating fluid boiling point: t_f = -10°C.

Freon heat capacity at constant pressure: c_p^f = 0.714 kJ/(kgK)

Inlet blast-furnace gas temperature: t_1 = 65 °C

Outlet blast-furnace gas temperature: t_2 = 35°C

Inlet blast-furnace gas humidity: d_1 = 250 g/m^3

Outlet blast-furnace gas humidity: d_2 = 54 g/m^3

We assume equipment size along the blast-furnace gas flow (depth) L = 400 mm suitable for accommodation of four serial banks of plate fins of 80x40 mm each. We assume as follows: fin thickness of δp = 0.4 mm, copper tube of 16x1 mm in diameter, fin pitch of S_p = 7 mm. Tubes are arranged in line with the same fin pitch in longitudinal and transverse directions $S_1 = S_2 = 0.04$ m (Figure 1).

Nominal fin height:

$$h = \frac{d_z}{2}\left(1.28\frac{S_1}{d_3}\sqrt{\frac{S_1}{S_2}-0.2}-1\right)\left(1+0.805*log\left(1.28\frac{S_1}{d_z}\sqrt{\frac{S_1}{S_2}-0.2}\right)\right) \quad (1)$$

where d_z is diameter of cooper tube.

$$h = \frac{0.016}{2}\left(1.28\frac{0.04}{0.016}\sqrt{1-0.2}-1\right)\left(1+0.805*\log\left(1.28\frac{0.04}{0.016}\sqrt{1-0.2}\right)\right) = 0.02 \text{ m}$$

Coefficient of frost build-up on the heat-transfer surface of equipment:

$$\varepsilon_{in} = 1+\frac{212.2\,(d_{bfg}-d_{fr})}{c_p^f\,(t_{bfg}-t_{fr})} \quad (2)$$

where d_{bfg} is average blast-furnace gas humidity , d_{fr} is rime humidity , t_{bfg} is blast-furnace gas temperature, t_{fr} is rime humidity.

$$\varepsilon_{in} = 1+\frac{212.2(\frac{152}{1.3}-15.4)}{714(50+12)} = 1.48$$

Blast-furnace gas side heat flux density:

$$q_p = \alpha_{bf}\varepsilon_{in}(t_{bfg}-t_{fr}) \quad (3)$$

where α_{bf} is blast-furnace gas heat-exchange coefficient.

$$q_p = 78.6*1.48*(50+12) = 7212\ W/m^2$$

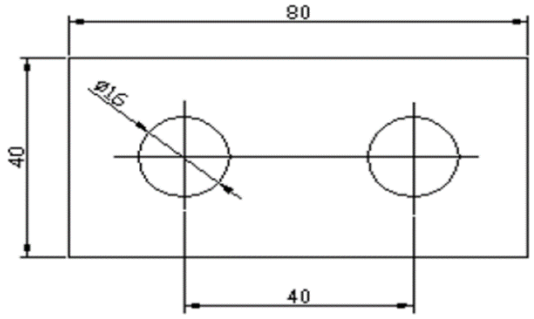

Figure 1 Plate fins

Nominal fin height:

$$\varepsilon_p = \frac{tah\left(\sqrt{\frac{2\ \alpha_{fr}}{\delta_p\ \lambda_p}}\ 0.02\right)}{\sqrt{\frac{2\ \alpha_{fr}}{\delta_p\ \lambda_p}}\ 0.02} \quad (4)$$

$$\varepsilon_p = \frac{tah\left(\sqrt{\frac{2*11.1}{0.0004*204}}\ 0.02\right)}{\sqrt{\frac{2*11.1}{0.0004*204}}\ 0.02} = 0.97$$

where λ_p is coefficient of thermal conductivity of the edge

$$\alpha_{fr} = \frac{1}{\frac{1}{\alpha_{bf}\ \varepsilon_{fr}}+\left(\frac{\delta_p}{\lambda}\right)_{fr}} \quad (5)$$

$$\alpha_{fr} = \frac{1}{\frac{1}{78.6*1.48}+\frac{1}{12.3}} = 11.1\ W/(m^2K)$$

Total finning efficiency can be calculated as follows:

$$\varepsilon_n = \varepsilon_p + (1-\varepsilon_p)\frac{f_{is}}{f_\Sigma} \quad (6)$$

where f_{is} is area of intercostal surface, f_Σ is total area of heat exchanger.

$$\varepsilon_n = 0.97+(1-0.97)\frac{0.048}{0.448} = 0.98$$

We determine evaporator heat-transfer surface as follows:

$$F_3 = \frac{Q_{ev}}{q_p} \quad (7)$$

where Q_{ev} is total heat flow

$$F_3 = \frac{1376*10^3}{7212} = 191\ m^2$$

Mass flowrate of refrigerating fluid under the complete boil-off condition:

$$M_f = \frac{4\,L^*\,q_p\,\beta}{d_{in}(i_{end}-i_{beg})} \quad (8)$$

$$M_f = \frac{4*10*7212*10.2*10^{-3}}{0.014*(701-488)} = 987\ kg(m^2 s)$$

where L^*- is pipe hose length, L^**=10 m* are refrigerating fluid enthalpies at the equipment inlet and outlet. According to the Freon boiling point R22 i_{beg} *= 488 kJ/(kgK)* and i_{end} *= 701 kJ/(kgK),*

β *is coefficient of finning*

d_{in}- inside tube diameter *16x2 mm* is 0.014 m;

Refrigerating fluid side heat-exchange coefficient:

$$\alpha_f = K\frac{M_f^{1.4}}{d_{in}^{0.5}} \quad (9)$$

$$\alpha_f = K\frac{987^{1.4}}{0.014^{0.5}} = 35772\ W/m^2K$$

where *K* is correction factor, we assume *K = 0.272.*

Mass flow of refrigerating fluid:

$$G_f = \frac{Q_{ev}}{i_{out}-i_{in}} \quad (10)$$

$$G_f = \frac{1376}{701-488} = 6.5\ kg/s$$

Total cross section available for refrigerating fluid passage

$$f_\Sigma = \frac{G_f}{M_f} \quad (11)$$

$$f_\Sigma = \frac{6.5}{986} = 6.6*10^{-3}\ m^2$$

Single tube nominal bore:

$$f_{tb} = 0.785 d_{in}^2 \quad (12)$$

$$f_{tb} = 0.785*0.014^2 = 1.54*10^{-4}\ m^2$$

Required number of coil sections:

$$n_c = \frac{f_\Sigma}{f_{tb}} \quad (13)$$

$$n_c = \frac{6.6*10^{-3}}{1.54*10^{-4}} = 43$$

Battery dimensions 2000x650x500 *mm*, suitable for installation of 2 fans.

Calculation of condenser for air heating is similar to that of evaporator. Finally, we obtain following results

Heat flux density is determined as:

$$q = k_{y\Sigma}(t_{gas} - t_{tb}) \quad (14)$$

where $k_{y\Sigma}$ is equivalent heat transfer coefficient.

$$q = 113*(50-40) = 565\ W/m^2$$

Value of equipment heat-transfer surface area:

$$F_z = \frac{Q_{ev}}{q} \quad (15)$$

$$F_z = \frac{1378*10^3}{1130} = 1219\ m^2$$

After inserting the necessary numerical values, let us apply these to 1 for determination of compressor power:

$$N = \frac{\rho_{fr}\,V_{fr}\,l_{fr}}{\eta_i\,\eta_m\,\eta_0} \quad (16)$$

where ρ_{fr} is freon density, V_{fr} is freon volume flow, l_{fr} is specific work, η_i is relative isothermal compressor efficiency (0.65 ÷ 0.85), η_m is mechanical efficiency of the compressor, η_0 is volume factor which takes into account freon volume losses due to leakage through compressor sealing intervals

$$N = \frac{15.4*0.42*16}{0.65*0.68*0.71} = 330\ kW$$

3 Determination of heat pump COP

COP is transformation coefficient showing the ratio of generated and thermal energy to electric power consumed by the heat pump. Coefficient can also be defined as the condenser heating effect to screw compressor power ratio.

Heat pump COP is determined according to following formula:

$$\eta_{COP} = \frac{Q_{con}}{N} \quad (17)$$

$$\eta_{COP} = \frac{1378}{330} = 4.2$$

Based on calculation of this heat pump COP, we come to conclusion that heat pump generates thermal energy 4.2 times as much as its electric power consumption for work execution.

4 Conclusions

The use of heat pump system for reduction of specific power consumption under the blast-furnace shop conditions is quite promising trend, and it can be applied at virtually every enterprise having blast furnaces.

Primary advantage of the proposed heat pump system is integration in the existing top gas treatment system. The proposed system does not require major reconstruction of existing equipment and features relatively small dimensions.

In addition to the primary objective of increasing the blast-furnace gas calorific power (due to the moisture content reduction), a few other serious practical problems are solved. One of such problems is increasing the temperature of combustion air supplied to hot-blast stoves. Sensible heat carried by air into the combustion zone allows calorimetric temperature increase by 3-5°C in the combustion zone, which would result in the blast-furnace air temperature increase and coke consumption reduction.

Furthermore, implementation of this system would enable production of substantial amount of the chemically purified water. The blast-furnace gas

cooling in the heat pump evaporator would yield up to 200g of H_2O per $1m^3$ of blast-furnace gas. This water could be further used in the blast-furnace shop cooling system.

5 The reference list

[1] KARP, I.N., ZAIVY, A.N.: Energy saving technologies in metallurgy, *Eenvironmental technologies and resource saving*, p. 13-20 2006.
[2] ROZENGART Y.I.: *Secondary energy resources of ferrous metallurgy*, Kyiv, High school, 1988.
[3] KARAKASH Y., GRES L.. Recirculation of waste gases in heat installations of agglomerate production *Acta Metallurgica Slovaca*, No. 3, pp. 135–138, 2000.
[4] KARAKASH Y., et all.,: New approaches to the creation of high-efficiency hot stoves, *Metalurgicheskaya teplotechnika*, No 1(16), pp. 65-71, 2009
[5] REAY, D., MACMICHAEL, D.: *Heat pumps. Design and applications Pergamon press*, Oxford, 1979
[6] KARAKASH Y., Gres L., Fleyschman Improving the energy efficiency of blast-furnace blast heating in blast furnaces in operation by installing a system of heat exchangers for heating the components of combustion and upgrading the air heaters, *Metal and casting of Ukraine*, No 5, Dnipro, 2014

Review process
Single-blind peer reviewed process by two reviewers.

Advances in Thermal Processes and Energy Transformation
Volume I, 2018, Knap01, p.19-22
ISSN 2585-9102

Laboratory investigation on thermal properties of recycled polyvinyl butyral

Lucia Knapčíková[1]

[1]*Department of Industrial Engineering and Informatics, Technical University of Košice, Faculty of Manufacturing Technologies with a seat in Prešov, Bayerova 1, 08001 Prešov, Slovakia, lucia.knapcikova@tuke.sk*

Category : Original Scientific Paper
Received : 28 January 2018 / Revised: 17 February 2018 / Accepted: 15 Marec 2018

Keywords : PVB, composites, environment, thermal analysi, DSC

Abstract : Nowadays, the use of secondary raw materials in the manufacturing process is a priority. With this it can be minimized entry investment and can be almost always succeeds as a perfectly substituting primary raw material. The use of polyvinyl butyral is large, and its advantage is a direct application to practice. The aim of this paper is thermal characterization of recycled polyvinyl butyral by differential scanning calorimetry. Using this analysis it was obtained results for Tg a Tm for a tested material. Recycled polyvinyl butyral is characterized by very good elasticity, adhesion to various surfaces, good water resistance, and high compatibility with other polymers and by good processing possibilities and possibility for application in many industries.

Citation: Knapčíková Lucia: Laboratory investigation on thermal properties of recycled polyvinyl butyral, Advance in Thermal Processes and Energy Transformation, Volume I, Nr 1(2018), p. 19-22, ISSN 2585-9102

1 Introduction

Thermal analysis refers to any technique for the study of materials which involves thermal control. Measurements are usually made with increasing temperature, but isothermal measurements or measurements made with decreasing temperatures are also possible. [1]. By the research was used a differential scanning calorimetry (DSC). This thermal analysis can also be used to follow the transfer kinetics of the tested material from a controlled release system into the bio membrane model. The advantage of using a calorimetric technique, compared to traditional release experiments, is the evaluation not only of the dissolution of the tested material released but also of the presence of a system able to take up the test sample released during the experiment, as well as of sample diffusion. [1]. The thermal properties of thermoplastic materials are equally as important as the electrical and mechanical properties. Unlike metals, thermoplastics are extremely sensitive to changes in temperature. The mechanical, electrical, and chemical properties of thermoplastics are dependent on the thermal properties at which the values were derived. The molecular chain crystalline has a number of important effects upon the thermal properties of a polymer. Semi-crystalline thermoplastics have a well-defined sharp melting point with thermo mechanical rigidity properties. Amorphous thermoplastics, in contrast, have a gradual softening range of the polymer melt. [2]The use of materials that are environmentally friendly is a priority for every industry. Polyvinyl butyral is characterized by good elasticity, adhesion to various surfaces, good water resistance, high compatibility with other polymers and also very good processing options, is becoming a priority material in this industry. [3]

2 Material definition

Polyvinyl butyral (PVB) is a special resin used as a raw material for glass laminated safety glass in cars and in the building industry, especially in high-rise buildings and, last but not least, in the photovoltaic industry, where is as solid coating form. PVB produces several companies in Europe, Asia and in USA, each under its trade mark [2]. Germany has become a powerhouse in the photovoltaic industry. The production of machines used for the production of components of photovoltaic installations and their equipment are mainly exported to Asia, except for Central and Eastern Europe. In addition to the main application and thus the use of PVB films, PVB resins are used for the production of paints, structural

adhesives, dry toner paints, and as binders for ceramics and composite fibers. [3] The PVB film has a number of outstanding features such as high tensile strength, impact resistance, transparency and flexibility, which is particularly useful in the production of safety glass. Consider of the alcohol, ester and acetate contents. [4]

Figure 1 Polyvinyl butyral in flakes form [9]

Due to the properties of polyvinyl butyral and its application in the many industries (primary in building, engineering, automotive industry), its primary use is mainly in the field of insulation. It is used as a special cover laminate film which forms a solid homogeneous whole on the insulations panels.
As we compared PVB with EVA by the solar energy using, currently, EVA (Ethylene-vinyl acetate) film is replaced with this thermoplastic. [5], [6] Compared to EVA foils, polyvinyl butyral has higher permeability, thus releasing light radiation with wavelength from 280 nm (EVA is 320 nm). [1]

Table 1 Material properties of polyvinyl butyral

Polyvinyl butyral (PVB)	
Form	flakes
Colour	neutral
Size	20-30 mm
Purity	more as 97%
Foreign mater content	less as 3%
Humidity	ca. 2%
Ratio of glass particles	less as 2%
Fire point	-
Melt point temperature	130 °C -170°C
Viskosity (dynamic)	100 – 175 m Pa*s (DIN 53015)

Polyvinyl butyral as a thermoplastic material is soluble in ethanol, butanol, ethyl acetate, butyl acetate, in a mixture of chlorinated hydrocarbons and is insoluble in aliphatic hydrocarbons (in petrol) The density of recycled polyvinyl butyral is 1,07g.cm^{-3} a and the recyclable sales price ranges from 0,25 € to 0,50 € per kilogram.
Translucent polyvinyl buyral (PVB) film is placed from the front and back of photovoltaic cells. The film melts, i.e., reaches the melting point Tm, thus filling all the gaps and removing the air between the layers. [6]

3 Thermal analysis of polyvinyl butyral

3.1 Diferential scanning calorimetry definition

By determining the glass transition temperature (Tg) and melting point (Tm) [7] for recycled polyvinyl butyral, important information about the processing possibilities of the test material is obtained. The method used in the test is called differential scanning calorimetry (DSC). [1] It belongs among the methods of thermal analysis and is suitable for measuring the characteristic temperature of the phase transitions I and II. heating. [4] It is also used to quantify the enthalpy characteristics associated with both physical and chemical changes of substances in the tested systems. This method can be used to measure the heat capacity, purity of substances and other special purposes.

3.2 Recycled polyvinyl butyral testing

Sample analysis took place under laboratory conditions at room temperature 22°C and humidity 60%, in accordance with standard DIN ISO 113 57. Laboratory equipment DSC 204 was used for analysis. Obtained datas were evaluated by NETZSCH Proteus. [94] The weight of the analyzed sample was 9 mg. The test temperature ranged from -50 °C to 300 °C. The measurement itself began by cooling the sample to -180 °C followed by heating. The run in key was -50°C.The sample is heated up to + 300°C. The following figure (Fig.2) looks at the device in which the analysis took place.

*Figure 2 Differential scanning calorimetry equipment **[9]***

Using the differential scanning calorimetry method [2],[6] the sample undergoes linear heating and hence the rate of heat flow in the sample. The heat flow is

proportional to instantaneous heat. Within the instrument, the internal temperature of which was equal to room temperature, (ca.20 ° C), two symmetric boxes were placed. The equipment is a resistive thermometer and a heating element that is embedded in the sample carrier and serves as the primary control of the system. The temperature of the sample is isothermal maintained with the comparison. Such amount of energy is needed to maintain isothermal conditions. [8] The process is plotted against time or temperature. Small samples (weight in mg) were used for analysis. The tested material is placed on metal pad, which reduce the thermal gradient to a minimum. As a result of the analysis, it was possible to use high heating rates (in tens of $K.min^{-1}$, $°C.min^{-1}$), thus ensuring a high resolution of the heating and the temperature range thus obtained. The following graphical representations obtained datas after DSC analysis of recycled polyvinyl butyral samples.

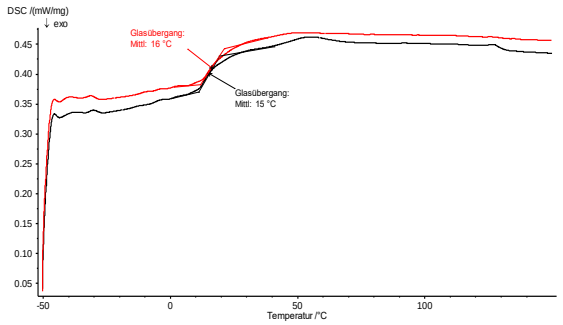

Figure 3 Results after differential scanning calorimetry measurement (1.Heating) [9]

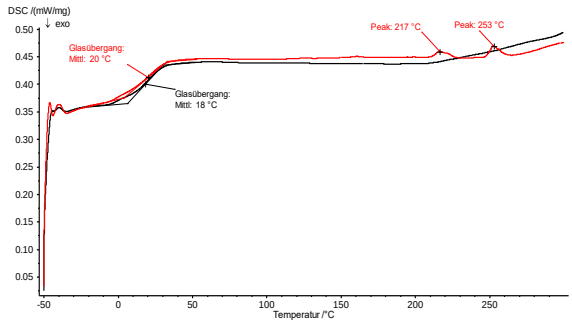

Figure 4 Results after differential scanning calorimetry measurement (2.Heating) [9]

Legend to the figures No.3 and No.4

From german language "Glasübergangstemperatur" - glass transition temperature (Tg)
Red color line - Recycled polyvinyl butyral (1.heating)
Black color line - Recycled polyvinyl butyral (2.heating)

From the graphical view that was obtained through the NETZSCH Proteus evaluation software there is a difference between the first and second heating. This means that during the first heating, to inaccurately place the sample in the test aluminium box. In the latter case, a final material analysis was obtained as such. Glass transition temperatures for recycled material range from 62 °C to 72°C. Melting point Tm is higher, temperature is about 150 °C. The value of 15 °C, the graph tells about the beginning of temperature changes in materials, but without disturbing the inner structure of the material.
Values at 217°C and 253°C point are presented violation of the inner bonding of the material. In view of the ongoing differential scanning calorimetry analysis, it can be concluded that the sample was deposited according to the rules of ca. 9 mg in an aluminium box and the results can be considered final. The advantage of using a differential scanning calorimetric technique, compared to traditional release experiments, is the evaluation not only of the dissolution of the tested recycled polyvinyl butyral released but also of the presence of a system able to take up the test sample released during the experiment, as well as of sample diffusion.

4 Conclusions

Polyvinyl butyral is used in the many industry for its:

- affordability,
- dielectric
- stability,
- low absorption and
- low water permeability.

The main reason is toxic harmlessness and chemical resistance. Due to its transparency, the recycled polyvinyl butyral sheet enables optical transmission in a given light spectrum region. Therefore, the use of this secondary raw material is now mostly advanced.
By determining the glass transition temperature (Tg) and melting point (Tm) temperature we obtained for recycled polyvinyl butyral an important information about the manufacturing possibilities.

5. The reference list

[1] WUNDERLICH, B. Thermal analysis.*Encyklopedia of materials:Science and Technology* [Online]Available on https://www.sciencedirect.com/topics/biochemistry-genetics-and-molecular-biology/thermal-analysis

[2] CAMPO, E.A. Thermal Properties of Polymeric Materials *Selection of Polymeric Materials.* [Online] Available on https://www.globalspec.com/reference/82025/203279/chapter-3-thermal-properties-of-polymeric-materials

[3] HUANG,X. et al. Thermal properties of polyvinyl butyral/graphene composites as encapsulation materials for solar cells, *Solar energy*, Vol.161, No.2,p.187-193,Available: Elsevier/ScienceDirect/S0038092X17311337 [19 February 2018].

[4] The use of risk assessment in environmental management,[Online] Available: eea.europa.eu [16 February 2018].

[5] ASIK, M Z. (2003)Laminated glass plates:revealing of nonlinear behavior. *Computers and Structures*, Vol.81, p.2659-2671

[6] LIU, B. H. et al. Systematic experimental study on mechanical behavior of PVB (polyvinyl butyral) material under various loading conditions. *Polymer Engineering and Science*, Vol.52, No.5, p. 1137–1147.

[7] DEL LINZ, P.et al. Reaction forces of laminated glass windows subject to blast loads. *Composites Structures*, Vol.131,s. 193–206, [04 February 2018].

[8] HOOPER P A, et al. On the blast resistance of laminated glass. *International Journal of Solids and Structures*, Vol.49, p.899–918, [03 March 2018]

[9] KNAPČÍKOVÁ L., Skúmanie materiálov na báze recyklovaného polyvinyl butyralu. Habilitačná práca. FVT TUKE, 2017. [Original in slovak].

Review process
Single-blind peer reviewed process by two reviewers.

Advances in Thermal Processes
and Energy Transformation
Volume I, 2018, Kuli01, p.23-26
ISSN 2585-9102

Study of the gaseous fuel combustion respect to the O_2 concentration and NOx formation

Andrii Kulikov[1] ● Marcel Fedák[1] ● Milan Abraham[1] ● Jakub Vahovsky[1]

[1.] *Department of Process Technique, Technical University of Košice, Faculty of Manufacturing Technologies with a seat in Prešov, Bayerova 1, 080 01 Prešov, Slovak Republic, andrii.kulikov@tuke.sk*

Category : Original Scientific Paper
Received : 27 January 2018 / Revised: 17 February 2018 / Accepted: 10 Marec 2018

Keywords : ANSYS, boiler, burner, combustion, simulation

Abstract : This paper dedicates thermodynamic and combustion processes respect to the NOx formation and O_2.concentration in the combustion air. Model of the boiler and the burners were made in the ANSYS 14.0. Results of the simulations have approved the results of the previous paper that increasing of the O2 concentration leads to the growth of the thermal equipment power but it has negative influence on the NOx production. Increasing of the O2 mass concentration by 1 % is leads to rising of the NOx by approximately 6 %.

Citation: Kulikov Andrii, et al.: Study of the gaseous fuel combustion respect to the O2 concentration and NOx formation, Advance in Thermal Processes and Energy Transformation, Volume I, Nr. 1(2018), p. 23-26, ISSN 255-9102

1. Introduction

Natural gas is one of the cleanest organic fuels, nevertheless it produces pollutants in combustion process. The major pollutants of the combustion in the atmosphere are carbon monoxide CO, nitrogen oxides NO, NO2, sulphur dioxide SO2 and hydrocarbons. The most toxic emissions are nitrogen oxides [1-3].

Nitrogen forms seven oxides, of which only monoxide and dioxide, NO and NO2, are dangerous pollutants, with dioxide being more dangerous than monoxide [4].

In natural conditions in the atmosphere, the amount of nitrogen oxides is measured in percentages. Nitrogen on the planet annually mobilizes about 140 million tons. Pollution by nitrogen oxides occurs both locally and globally [5-8].

In the current article were made the simulations of the industry gas burner which are installed in the high-pressure boilers.

2. Model description

To understand and calculate the mechanism of the NOx formation the CFD simulations were made. Combustion processes were calculated in the ANSYS Fluent 14.0 [9].

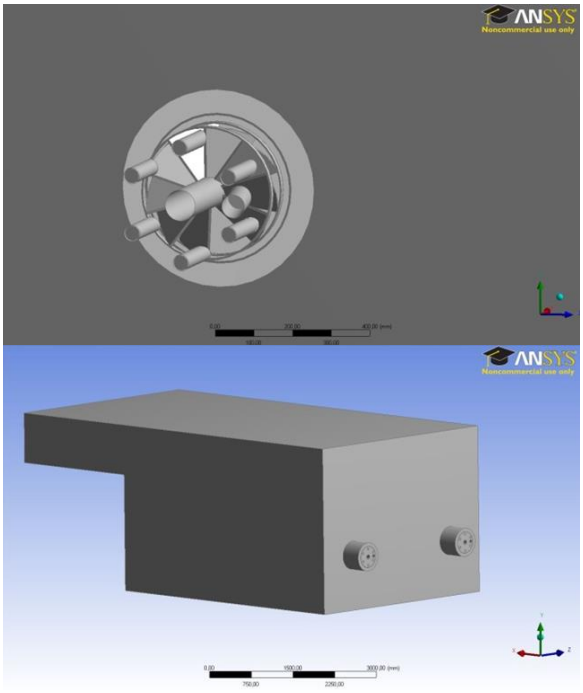

Figure 1 ANSYS models of the boiler and burners

The models of the 30 MWh boiler and two 15.7 MWh burners are in the figure 1. The model was made in the integrated to the ANSYS module Design Modeler. The redrawn geometry of the burner was simplified to decrease the numbers of the elements in the mesh to reduce calculation time of the simulation. Nevertheless any changes in the geometry must not

influence thermodynamics or chemistry processes in the boiler. Total number of the elements in the model mesh is 7 946 439. Example of the generated mesh is in the figure 2.

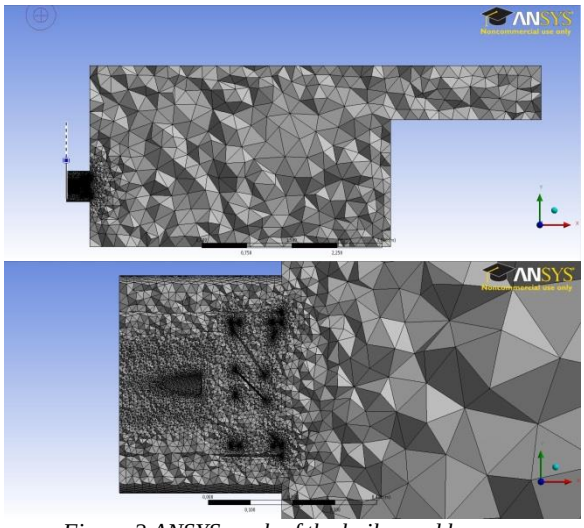

Figure 2 ANSYS mesh of the boiler and burners

Parameters of the mesh generation (proximity and curvature advanced size function) were selected for the best definition of the different planes and volumes.

3. Simulation

To understand the thermos mechanical processes inside the boiler simulation of the non-premixed combustion was made. All input physical parameters were chosen according to the normal operation conditions of the boiler and the burners.

Simulations of non-premixed combustion were made with the fuel of average composition for 2017 year according to the SPP report (Table 1).

Tab. 1 Composition of the fuel

Natural gas composition [mol,%]	
Methane	95,361
Etan	2,6231
Propane	0,6437
Butane	0,8504
Pentane	0,0407
Hexane + other	0,0255
Carbon dioxide	0,3788
Nitrogen	0,7205

The air composition is in the table 2.

Tab. 2 Composition of the air

Element	Volume [%]
N2	0,79
O2	0,21

Results of the simulation are in the figure 3.

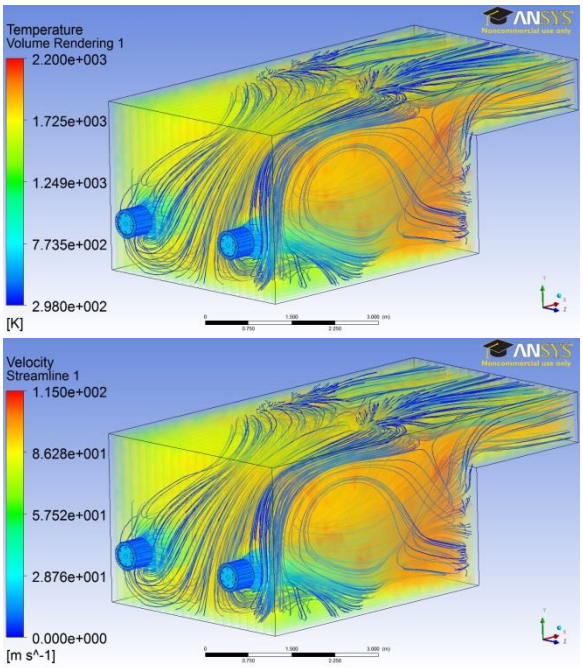

Figure 3 Results of the simulation (temperature and velocity)

At the upper part of the figure 3 is shown temperature volume rendering. At the dawn part of the figure 3 is shown velocity streamlines of the inlet mases.

According to the results of the simulation the maximum temperature inside the boiler is 1931 K. The areas of the maximum temperature are situated near the wall in front of the burners. Average temperature inside the boiler is 1705 K.

According to the simulation there is a good circulation of the hot gaseous mases inside the combustion chamber (aprx. 3-5 times).

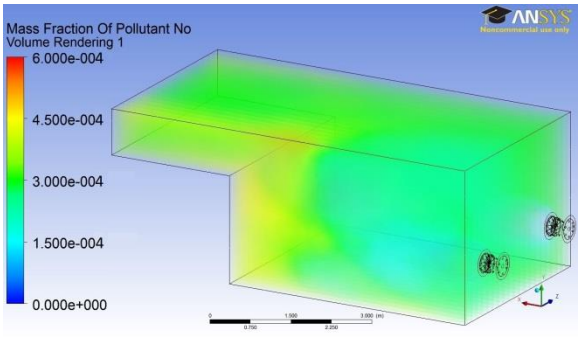

Figure 4 Results of the simulation (NOx)

Figure 4 represents mass fraction of the NO. Maximum concentration of the NO in the boiler is 182 ppm. The average concentration inside the combustion chamber is 89 ppm, concentration at the exhauster is 138 ppm. From the EU legislative the maximum possible NOx exhausting for such thermal equipment is 250 ppm (taking to account year of reconstruction and burners type).

According to the results the most of the NO is produced at the end of the flame, close to the wall. As it is represented in the figure 4 the thermal NOx are the main source of the pollutants. Figure 5 represent simplified scheme of the NOx formation.

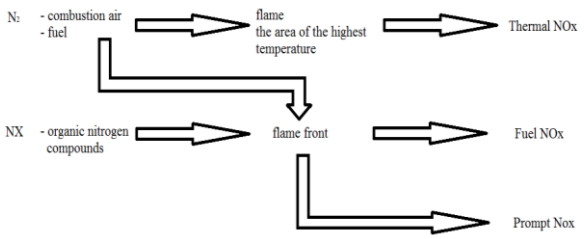

Figure 5 simplified scheme of the NOx formation.

Thermal NOx produces majorly in the flame front and areas of the high temperatures so their production is controlled by the nitrogen and oxygen molar concentrations and the temperature of combustion. According to the Arrhenius formulation combustion at more than 1,500 K exponentially increase concentrations of thermal NOx.

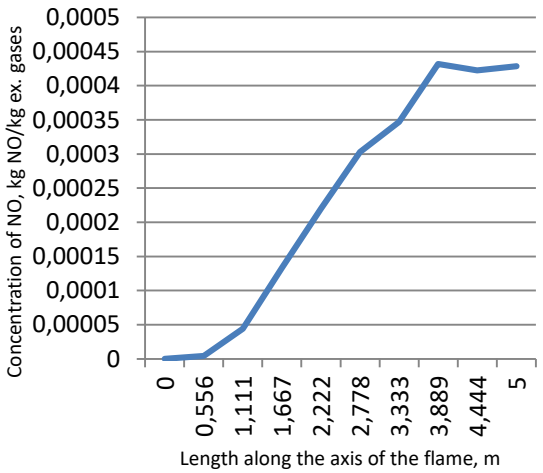

Figure 6 Concentration of the NO along the flame axis

Figure 6 represents concentration of the NO along the flame axis. According to the results of the simulation length on the flame is around 2,5 - 3 m. As it is shown in the figure 6 concentration of the NO increased exponentially along the flame axis (from 0 to 3 m). Next area from the flame end to the wall is characterises as an area of high temperatures where NO production is also majorly controlled by the Arrhenius formulation.

There is equipment which is installed in the burner to inject O2 to the air to increase the power of the boiler and this way to cover the maximum heat consumption.

The simulation with higher O2 concentration was made with next air composition (tab 3).

Tab. 2 Composition of the air with higher O2 concentration

Element	Volume [%]
N2	0,78
O2	0,22

The results of the simulation of the boiler with higher O2 concentration in the air are in the figure 7

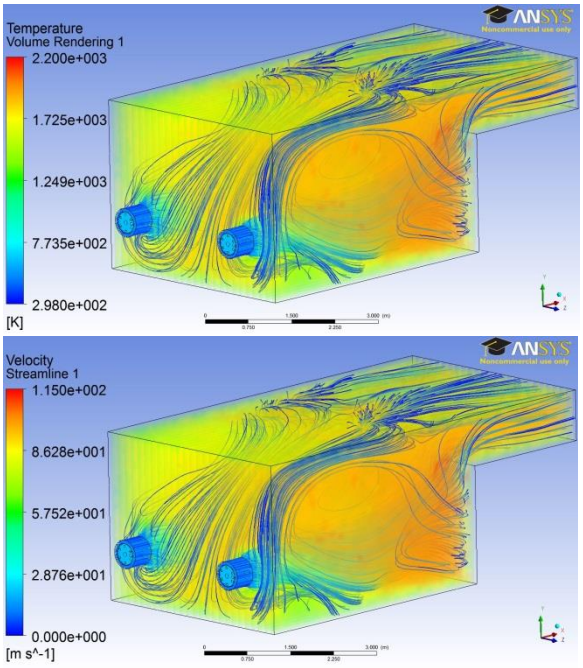

Figure 7 Results of the simulation (temperature and velocity with higher O_2 concentration.)

At the upper part of the figure 7 is shown temperature volume rendering. At the dawn part of the figure 3 is shown velocity streamlines of the inlet mases.

According to the results of the simulation the maximum temperature inside the boiler rise by 5,7 % to 2041 K comparing with the simulation with lower O2 concentration. The areas of the maximum temperature are situated near the wall in front of the burners. Average temperature inside the boiler is also increased by 6,2 % to1811 K.

According to the simulation there is still good circulation of the hot gaseous mases inside the combustion chamber (aprx. 3-5 times).

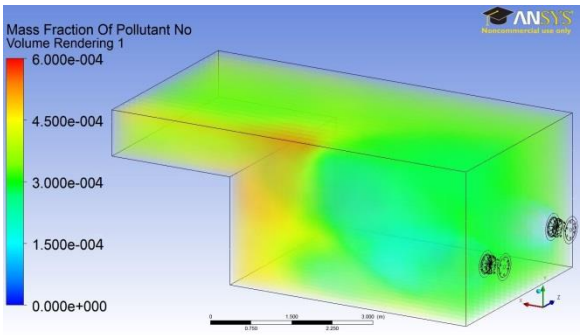

Figure 8 Results of the simulation (NOx with higher O_2 concentration)

Figure 8 represents mass fraction of the NO. Maximum concentration of the NO in the boiler increased by 6,04 % to 193 ppm comparing with the simulation with lower O2 concentration. The average concentration inside the combustion chamber has risen up to 95 ppm, concentration at the exhauster - to 145 ppm. Figure 9 represents concentration on the NO along the flame axis.

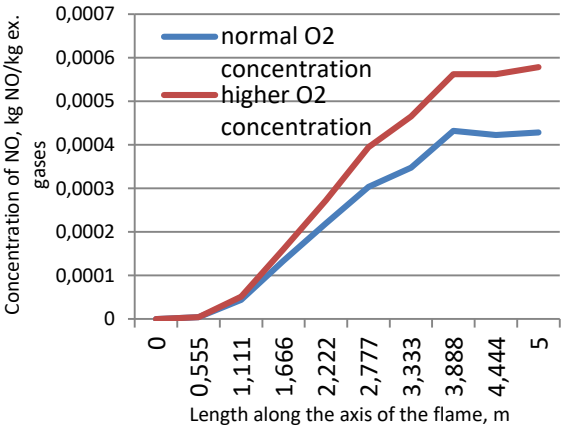

Figure 9 Concentration of the NO along the flame axis

According to the figure 9 increasing of the O2 mass concentration by 1 % leads to rising of the NOx by approximately 6 % in the current working thermal characteristics of the boiler as the thermal load of the combustion chamber is placed in the Arrhenius formulation border.

Conclusions

Above theoretical and experiential knowledge which allows understanding and calculating the mechanisms of NOx formation in the high-pressure boilers. Also the main management points of control of the thermal machines respect to its efficiency and ecological problems are presented.

Simulations confirm the mechanism of the NOx formation according to the Arrhenius formulation in the thermal equipment with high thermal load of the combustion chamber. Increasing of the O2 mass concentration by 1 % is leads to rising of the NOx by approximately 6 %.

Nevertheless it is possible to increase the power of the thermal equipment by rising of the O2 concentration in the combustion air.

The reference list

[1] RIMÁR M., FEDÁK, M.,: Combustion processes. Presov 2014.

[2] ŠMERINGAI, P., et al.: Optimization of combustion process with respect to the assessment of nitrogen oxides formation, *Energy transformations in industry*. Košice, pp. 190-194., 2015.

[3] ŠMERINGAI, P., RIMÁR, M.,: Process simulation in combustion plants with a few industrial burners In: *Management of Manufacturing Systems 2014*, pp. 116-119., 2014.

[4] VARGA A., et al.: The oxidant in the combustion process, 1st ed., Košice, 2015.

[5] RIMAR, M., JUMP, P.,: Thermodynamics, Prešov University, FVT, 2013.

[6] DZURŇÁK R., et al.: Simulation of the gaseous fuels burning by CFX software, *Seminar on energy process*, Košice, 2015.

[7] PANDA, A., et al.: Progressive technology diagnostic and factors affecting to machinability. *Applied Mechanics and Materials*, Volume 616, pp. 183-190. 2014.

[8] ZAJAC J., ČORNÝ I.,: Monitoring of processing fluids. *Science Report*, Kielce, pp. 215-229, 2004.

[9] GAVLAS S, et al.: Design and numerical simulation of the heat exchanger for heat recovery system with melting furnaces for melting secondary aluminums, EFM12 Experimental Fluid Mechanics, 2012.

Acknowledgement

This work was supported by the Slovak Research and Development Agency under the contract No. APVV-16-0192